Korean J. of Chem. Eng., 12(5), 503-511 (1995)

EXPERIMENTAL AND THEORETICAL STUDY ON H_2/CO_2 SEPARATION BY A FIVE-STEP ONE-COLUMN PSA PROCESS

Wang-Gi Kim, Jaeyoung Yang, Sangsup Han, Chanhwi Cho*, Chang-Ha Lee† and Hanju Lee

Dept. of Chem. Eng., College of Engineering, Yonsei University, Seoul, Korea
*Dept. of Chem. Eng., Youngdong Institute of Technology, Youngdong, Korea
(Received 18 January 1995 • accepted 22 July 1995)

Abstract—An experimental and theoretical study is performed for bulk separation of H_2/CO_2 mixture (70/30 volume %) by PSA process with zeolite 5A, a process widely used commercially in conjunction with the catalytic steam reforming of natural gas or naphtha. For the optimized adsorption conditions of PSA, the characteristics of adsorption/desorption characteristics have been studied through breakthrough and desorption experiments under various conditions. The purge-to-feed ratio is important to the H_2 product purity only at a long adsorption step time. H_2 could be concentrated from 70% in the feed to 99.99% at H_2 recovery of 67.5%. The results of all five steps in PSA are successfully predicted by the LDF model considering an energy balance and nonlinear isotherm. For the model, the effective diffusivities (D_e) are obtained separately from the uptake curves of H_2 and CO_2. The Langmuir-Freundlich isotherm is used to correlate the experimental equilibrium data and is very well fitted to the results.

Key words: *Pressure Swing Adsorption, H_2/CO_2 System, LDF Model, P/F Ratio, Adsorption Time*

INTRODUCTION

Separation and purification of gas mixtures by pressure swing adsorption (PSA) technology has become an important unit operation in the chemical industry. A large variety of binary and multicomponent gas mixtures are commercially being separated using this technology [Ruthven, 1984; Yang, 1987]. One of the promising applications of PSA is to purify the crude H_2 stream in catalytic steam reforming of natural gas or naphtha by selective adsorption of the impurities on solid adsorbents such as zeolites, due to the increasing demand for hydrogen in petroleum refining and petrochemical industry [Stewart and Heck, 1969; Yang, 1987; Haung and Fair, 1988]. Typical reformer off-gas consists of H_2 (77%), CO_2 (22%), and other small amount of impurities (less than 1%).

In PSA the adsorber is regenerated by rapidly reducing the partial pressure of the adsorbate, that is, lowering the total pressure or additionally using a purge gas. PSA was originally invented by Skarstrom [1959] and is modified by many scientists/engineers and various modifications have been reviewed extensively [Wankat, 1986; Yang, 1987]. The aim of such modifications varies, but they basically try to improve the performance of the apparatus by changing the plant configuration as well as the operating scheme. One way of improving the efficiency of the system is to modify some parameters of the process, such as the pressure ratio, the purge-to-feed ratio, the cycle time, the particle and column diameter, and so on. However, it is often difficult to understand the reasons for high productivity in PSA, since the effects of process parameters are strongly related to one another. Therefore, there have been publications recently on the study of the process by modeling or simulation. Most of the PSA models are based on the simplest equilibrium theory [Cheng and Hill, 1983; Fernandez and Kenney, 1983]. Whereas for the air-drying PSA process, Carter and Wyszynski [1983] have accounted for the mass transfer rates in porous sorbent using the linear driving force approximation. All of these models used the linear isotherms. However, the important features of bulk gas separation by zeolites are the nonlinearity of the adsorption isotherms, the variation of gas velocity in the column, and large temperature excursions during each cycle, all of which increase the complexity of the model.

Recently, several experimental studies and theoretical models considering these features in pore diffusion model (PDM) [Yang and Doong, 1985; Liow and Kenney, 1990; Lu et al., 1992; Kikkinides et al., 1993] or linear driving force (LDF) model [Cen and Yang, 1986; Kapoor and Yang, 1989; Ritter and Yang, 1991] have been published. However, Ruthven [1984] points out that the constant-diffusivity micropore diffusion model using calibrated effective diffusivities is no better than an LDF model using the limiting diffusivity. In view of the computational efficiency, the LDF approach appears preferable at this stage.

This paper describes experimental and theoretical results of separation of H_2/CO_2 mixtures by PSA with zeolite 5A as the adsorbent, because crude hydrogen stream from a steam reformer contains a significant quantity of carbon dioxide. The theoretical model considering the effects of heat of adsorption has been developed for a five-step PSA cycle (pressurization, adsorption, cocurrent depressurization, countercurrent blowdown, light-product purge) in a single bed. The effects of adsorption time and purge-to-feed (P/F) ratio in PSA are also investigated. The adsorbent chosen in this study is zeolite 5A, since the zeolite 5A have the higher selectivity for CO_2. Pure gas adsorption isotherms and diffusion rates for zeolite 5A are independently measured and used as physical data in the model. The linear driving force (LDF) model [Glueckauf, 1955] for mass transfer rates and the extended Langmuir-Freundlich equations for mixed gas isotherms are incorporated in this model. The model is used to study the bed dynamics in both the transient and cyclic steady-state regimes, as

†To whom all correspondence should be addressed.

well as to predict the overall process performance.

MATHEMATICAL MODEL

For developing a dynamic model of adsorption column, sets of mass and energy balances, the adsorption rate equation, and equilibrium isotherms must be considered. To simplify the derivation and calculation, the following assumptions and approximations are made:

1. The ideal gas law applies.
2. The axial pressure gradient across the bed is neglected.
3. Plug-flow condition holds; i.e., axial dispersion is neglected.
4. Thermal equilibrium is attained all the time between the bulk fluid and the particles.
5. No variation exists in the radial direction for both concentration and temperature.
6. Transport (D_e in LDF model) and physical properties are assumed to be independent of temperature.

The mass balance equation for component i in the adsorption column are given by:

$$\alpha\frac{\partial C_i}{\partial t}+\frac{\partial uC_i}{\partial z}+\rho_B\frac{\partial \bar{q}_i}{\partial t}=0 \text{ where } i=1, 2, 3,\cdots,n \tag{1}$$

where C_i is the concentration of component i in bulk flow and α is the interparticle void fraction. The velocity, u, is the superficial velocity. This equation can be rewritten into an overall mass balance [Eq. (2)] and component [Eq. (3)] equations:

$$\frac{\alpha}{RT}\frac{\partial P}{\partial t}-\frac{\alpha P}{RT^2}\frac{\partial T}{\partial t}+\frac{P}{RT}\frac{\partial u}{\partial z}-\frac{uP}{RT^2}\frac{\partial T}{\partial z}+\sum_{j=1}^{n}\rho_B\frac{\partial \bar{q}_i}{\partial t}=0 \tag{2}$$

$$\frac{\alpha P}{RT}\frac{\partial y_i}{\partial t}+\frac{uP}{RT}\frac{\partial y_i}{\partial z}-y_i\sum_{j=1}^{n}\rho_B\frac{\partial \bar{q}_i}{\partial t_j}+\rho_B\frac{\partial \bar{q}_i}{\partial t}=0 \text{ where } i=1,2,\cdots,n-1 \tag{3}$$

Appropriate adsorption rate into the adsorbent, $\partial\bar{q}_i/\partial t$, is crucial in simulating the adsorption process. Assuming spherical shape and uniform radius of adsorbent, the intraparticle diffusion equation for each species, i, becomes

$$\frac{\partial q_i}{\partial t}=D_e\frac{1}{r^2}\frac{1}{\partial r}\left(r^2\frac{\partial q_i}{\partial r}\right) \tag{4}$$

With a assumption of parabolic concentration profile within the adsorbent, adsorption rate can be represented by the linear driving force (LDF) model and written by:

$$\frac{\partial \bar{q}_i}{\partial t}=\frac{15D_e}{R_p^2}(q_i^*-\bar{q}_i) \tag{5}$$

where q_i^* is an amount of adsorption of component *i* in equilibrium state of mixture.

The Langmuir-Freundlich isotherm is used to correlate the experimental single component adsorption isotherm. The isotherms then can be extended for predicting the multicomponent isotherm by the following loading ratio correlation (LRC) equation [Eq. (6)] as:

$$q_i=\frac{q_{mi}B_iP_i^{n_i}}{1+\sum_{j=1}^{n}B_jP_j^{n_j}} \tag{6}$$

The isotherm parameters are functions of temperature and are described as:

$$q_m=k_1+k_2T$$
$$B=k_3\exp(k_4/T)$$
$$n=k_5+k_6/T \tag{7}$$

Since the bed is not isothermal in the bulk separation, the following energy balance for the bed is necessary:

$$(\alpha'\rho_gC_{pg}+\rho_BC_{ps})\frac{\partial T}{\partial t}+\rho_gC_{pg}u\frac{\partial T}{\partial z}-\sum_{j}^{n}Q_i\rho_B\frac{\partial \bar{q}_i}{\partial t}+\frac{2U_i}{R_{Bi}}(T-T_0)=0 \tag{8}$$

where α' is the total void fraction. The last term is necessary to account for the heat transfer through the column wall and U_i in this term is an overall heat transfer coefficient based on internal column area:

$$U_i=\frac{1}{\frac{1}{h_i}+\frac{x_w}{k_w}\left(\frac{D_i}{\overline{D}_L}\right)+\frac{1}{h_o}\left(\frac{D_i}{D_o}\right)} \tag{9}$$

where h_i and h_o are surface heat transfer coefficient for inside and outside the column, respectively, and k_w is the thermal conductivity of the column wall.

The boundary conditions for the PSA cycle are:

Step I(Pressurization): $y_i(t,0)=y_{i,0}$, $T(t,0)=T_0$, $P=P(t)$, $u(t,L)=0$
Step II(Adsorption): $y_i(t,0)=y_{i,0}$, $T(t,0)=T_0$, $P=P_A$, $u(t,0)=u_{feed}$
Step III(Cocurrent depressurization): $P=P(t)$, $u_i(t,0)=0$
Step IV(Countercurrent blowdown): $P=P(t)$, $u_i(t,L)=0$
Step V(Light product purge): $P=P(t)$, $u(t,L)=u_{purge}$

The pressure history, P(t), as recorded by pressure transducer, is used as the boundary condition in the form of polynomial function matched with recorded data.

The model equations (overall mass balance [Eq. (2)], component mass balance [Eq. (3)], energy balance [Eq. (8)], adsorption rate equation [Eq. (5)]must be solved simultaneously with input parameters described above to predict the breakthrough/desorption curve or to simulate PSA processes. The adsorption rate equation [Eq. (5)] is first calculated. With the value of adsorption rate, the superficial velocity is calculated from the overall mass balance equation [Eq. (2)]. Finally, with the values obtained above, component mass balance [Eq. (3)] and energy balance [Eq. (8)] are solved to obtain composition of components and temperature of the column, respectively.

In many studies of PSA, the model equations are generally solved by employing finite difference methods with an implicit Euler method of a Crank-Nicolson method to ensure stability. However, these methods still show the problem of numerical oscillation in the discontinuous points. In this study, the partial differential equations representing the packed column are solved by the flux corrected third-order upwind method. Numerical oscillation, which often appears when convection equation is solved, is eliminated by the flux corrected scheme (FCS). The number of axial grid nodes used is 100 per 100 cm length.

EXPERIMENTAL SYSTEM AND PROCEDURES

1. Apparatus and Materials

A schematic diagram of the one-column PSA unit is shown in Fig. 1. The adsorption column is a stainless steel pipe 100 cm

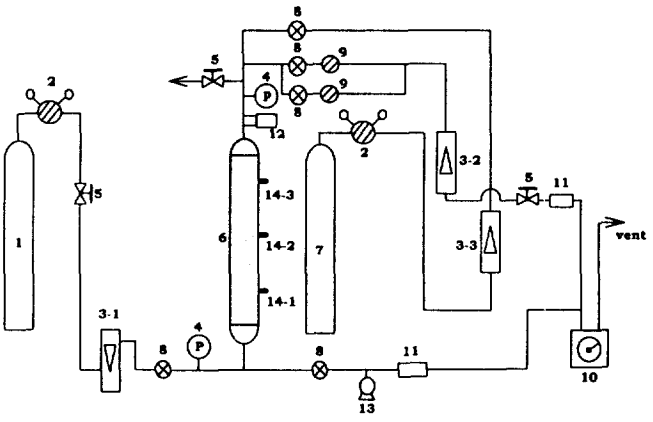

Fig. 1. Schematic diagram of apparatus for a single column pressure swing adsorption process.

1. Feed gas cylinder
2. Pressure regulator
3. Flowmeter
4. Pressure gauge
5. Needle valve
6. Adsorption bed
7. Purge gas cylinder
8. Solenoid valve
9. Back pressure regulator
10. Wet test meter
11. Sampling port
12. Pressure transducer
13. Vacuum pump
14. Resistance temperature detector

Table 1. Characteristics of adsorbent and adsorption bed

Adsorbent	
Form	zeolite 5A(sphere)
Nominal pellet size	4-8 mesh
Average pellet size	$R_p = 1.57$ mm
Pellet density	$\rho_p = 1.16$ g/cm^3
Intracrystal void fraction	$\varepsilon_c = 0.29$
Macropore void fraction	$\varepsilon_a = 0.36$
Average macropore radius	$R_a = 986$ Å
Average heat capacity	$C_{ps} = 0.22$ cal/g K
Weight fraction of crystals	$\omega = 0.83$
Adsorption column	
Inside radius	$R_{Bi} = 1.1$ cm
Outside radius	$R_{Bo} = 1.275$ cm
Wall thickness	$x_w = 0.175$ cm
Bed length	$L = 100$ cm
Wall heat capacity	$C_{pw} = 0.12$ cal/g K
Bulk (bed) density	$\rho_B = 0.795$ g/cm^3
External (interpellet) void fraction	$\alpha = 0.315$
Total void fraction	$\alpha' = 0.76$

long and 2.2 cm I.D. The adsorbent is 4-8 mesh zeolite 5A, manufactured by Davison Chemical Division of the W. R. Grace Co. The glass wool is compressed on top of the bed to prevent the carryover of particles. The characteristics of zeolite 5A and column are shown in Table 1. All connecting lines are a quarter-inch stainless steel tubing. Solenoid valves are installed to direct the flow into and out of the column. These solenoid valves are controlled by a computer, which runs the control program to operate at desired time cycles. High pressure in the bed is controlled by a back-pressure regulator (Tescom Co.), and the low pressure is atmospheric. Pressure transducer outside the top of the column is installed to acquire the pressure history of the process. The

Table 2. Each step time and P/F ratio for five-step PSA experiment*

	Step time (s)					P/F ratio
	Step I	Step II	Step III	Step IV	Step V	
run A	60	360	60	90	180	0.029
run B	60	360	60	90	180	0.052
run C	60	360	60	90	180	0.100
run D	60	240	60	90	180	0.029
run E	60	240	60	90	180	0.052
run F	60	240	60	90	180	0.100

*pressure: step I (from 1 atm to 11 atm), step II (11 atm), step III (from 11 atm to 8.4 atm), step IV (from 8.4 atm to 1 atm), and step V (1 atm)

axial temperature is measured with three thermocouples (RTD), which lay at 10 cm, 50 cm, and 80 cm from the feed end. These data of temperature and pressure are recorded by a computer using A/D converter. Gas samples are taken from the light product (H_2) and heavy product (CO_2) lines and analysed with a thermal conductivity detector (TCD).

2. Procedures

The procedure described below is for bulk separation of a H_2/CO_2 (70/30 volume %) mixture. The bed is cleaned before breakthrough experiments and each run of PSA processes by degassing with a mechanical vacuum pump. Step I, pressurization, is initiated by opening the bottom valve (8-1) connected to a feed tank and the bed is pressurized to the adsorption pressure, 11 atm. The desired column pressure is controlled by the pressure regulator connected to the feed gas cylinder. Step II, high-pressure adsorption, starts when the top product valve (8-4) is opened. The flowrate in step II is controlled by adjusting a metering valve in the feed line. Step III, cocurrent depressurization, is effected by closing the feed valve (8-1) and opening the valve (8-3) in the side stream line of light product. The metering valve in this side stream line controls the rate of cocurrent depressurization. The column pressure drops to 8.4 atm in this step. Step IV. countercurrent blowdown, is achieved by simultaneously opening the bottom valve (8-2) in the exhaust line and closing the valve (8-3) in the side stream line. When the column pressure drops to atmospheric pressure, the solenoid valve (8-5) in the H_2 purge line opens and starts light product (H_2) purge. The H_2 gas used in this step is pure hydrogen whose purity is 99.9%.

The PSA experiments are designed to study the effects of purge/feed (P/F) ratio and adsorption time on separation. Two cycle times are used. For runs A, B, and C, step time intervals are 60 s (step I), 360 s (step II), 60 s (step III), 90 s (step IV), and 180 s (step V), respectively. For runs D, E, and F, time intervals are the same except for step II (240 s). The cycle step times affect the performance of PSA process such as purity and recovery greatly. But these cycle step times are selected rather arbitrarily for the simulation study. These step time intervals are not optimal step times for H_2 separation PSA process, but would change for the actual multibed PSA process. A cyclic steady state is generally reached after 10 cycles. To study the desorption by a purge gas, adsorption column which had been saturated by H_2 or CO_2 at 1 atm is purged by He gas. All experiments are performed at ambient temperature and at a constant feed rate. The experimental conditions and process characteristics are summarized in Table 2.

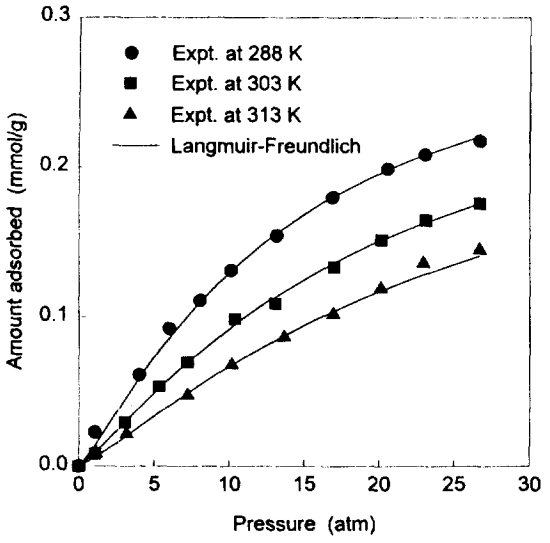

Fig. 2. Adsorption isotherms of H_2 at several temperatures on 5A zeolite.

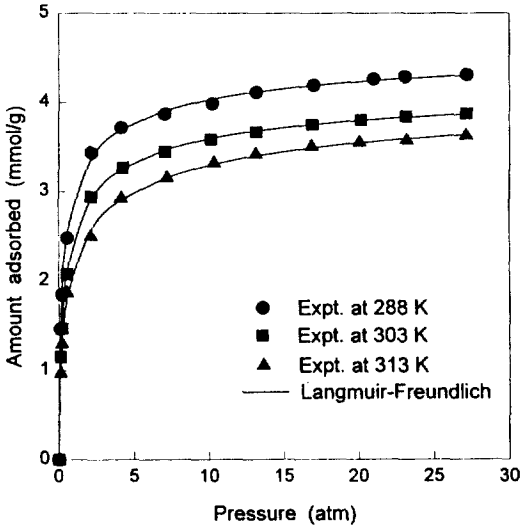

Fig. 3. Adsorption isotherms of CO_2 at several temperatures on 5A zeolite.

RESULTS AND DISCUSSION

The main objective of the study is to develop an optimized PSA cycle which can produce high purity H_2 in the adsorption product with a maximum yield. The main parameters that describe the performance of a PSA process are the purity as well as the yield of H_2 product. Definitions of the above parameters can be found elsewhere [Yang, 1987].

1. Model Input Parameters and Method of Solution

The following information is needed for the model: equilibrium parameters, heat transfer coefficient, heat of adsorption, and diffusivities of each components. Equilibrium isotherms for H_2 and CO_2 gas are measured by the volumetric method at 288-313K and 0-30 atm. Fig. 2 and 3 show that the experimental data are very well fitted by the Langmuir-Freundlich isotherm. The results as expected show a very high selectivity for CO_2 over H_2 at the range of experimental temperatures. The selectivity ratio decreases as temperature increases, because of the stronger physical bonds of CO_2 with zeolite 5A, which results in a much higher heat of adsorption for CO_2, compared to that for H_2. From single component isotherm parameters, temperature-dependent parameters, Eq. (7), for adsorption of mixture are obtained by matching the experimental data with Langmuir-Freundlich isotherm. The parameters are listed in Table 3. The isosteric heat of adsorption is obtained by using the Clausius-Clapeyron equation as following.

Table 3. Temperature dependence functions' parameters of extended Langmuir-Freundlich isotherm and heat of adsorption

Gas	k_1 (mmol/g)	k_2 (mmol/g K)	k_3 (1/atm)	k_4 (K)	k_5 (−)	k_6 (K)	Q (cal/mol)
H_2	4.314	−0.01060	0.002515	458.2	0.9860	43.03	2800
CO_2	10.03	−0.01858	0.2781	207.2	−5.648	2098	7200

$$\left[\frac{d\ \ln P}{d\left(\frac{1}{T}\right)}\right]_q = -\frac{Q}{R} \tag{10}$$

Since overall heat transfer coefficient (U_t) varies only slightly with column temperature, a constant value is used in the model. The estimated value used in this study is 1.469×10^{-4} cal/cm²·K·s.

The thermogravimetric analysis (TGA) technique is used to measure uptake curves of H_2 and CO_2 at 25℃ and 1 atm. High purity He is used as the inert carrier gas and the gas for regeneration. From this result, effective diffusivity for the LDF model is obtained by matching experimental uptake curve with theoretical uptake curve using the homogeneous solid diffusion model. Those values are 9.646×10^{-4} cm²/s and 9.421×10^{-5} cm²/s for H_2 and CO_2 gas, respectively. The effective diffusivity is assumed to be independent of surface coverage since at low pressures this dependence is generally very weak [Kikkinides et al., 1993]. For equilibrium controlled separation process such as H_2/CO_2 system, kinetic effect is only of secondary importance and give very little change in performance under the condition the system is operating close to equilibrium [Farooq and Ruthven, 1991; Ruthven et al., 1994]. Thus, the LDF model with constant diffusivities which were determined under a limited condition (1 atm and 25℃) could be used to predict the equilibrium controlled separation.

2. Adsorption/desorption Dynamics of Adsorption Column

In order to optimize the performance of the adsorption tower it is foremost important to understand the characteristics of adsorbent and adsorbate interactions in terms of thermodynamics and kinetics. One of the methods to analyse these characteristics is to compare the observed change of concentration and temperature profiles vs. time with theoretically calculated results. Such confirmation of concentration and temperature breakthrough curve can be in itself one of the goals of this study or it can be used as a basic data for optimization of a PSA process. The dynamics of an adsorption column are affected by several factors and the most prominent factors are the geometry of the adsorption column, the operating conditions, the characteristics of mass transfer, the effects of adsorption heat, and the type of adsorption equilibrium isotherm.

2-1. The Effects of Feed Velocity on Breakthrough Curves

Fig. 4 shows the effects of feed velocity on breakthrough cur-

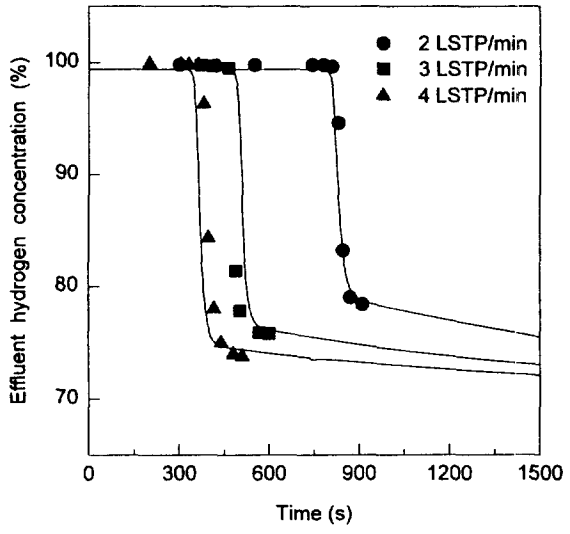

Fig. 4. Effect of feed flow rate on breakthrough curves predicted by LDF model at 6 atm.

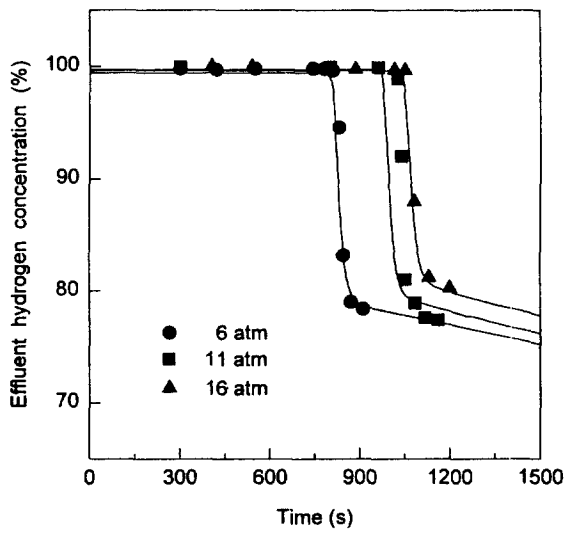

Fig. 5. Effect of adsorption pressure on breakthrough curves predicted by LDF model at constant feed rate, 2 LSTP/min.

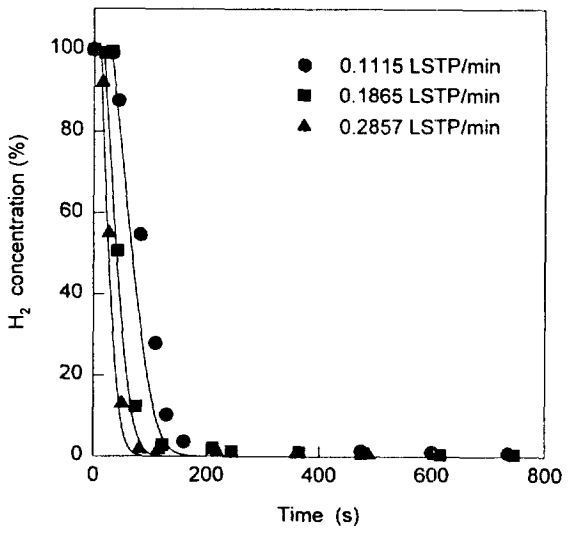

Fig. 6. Desorption of H_2 with He gas at several purge flow rates.

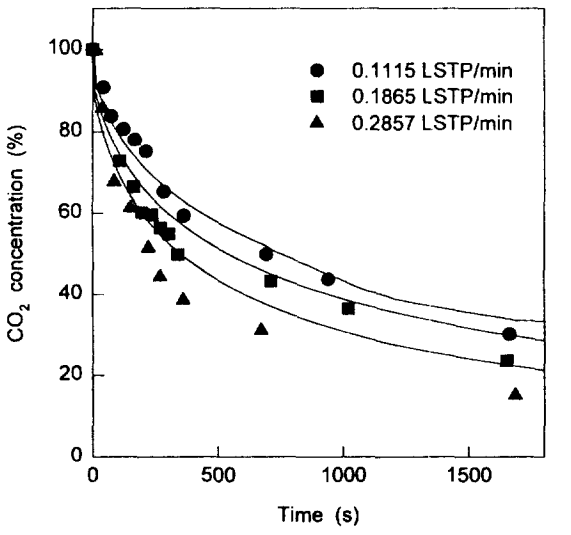

Fig. 7. Desorption of CO_2 with He gas at several purge flow rates.

ves. The slower the feed velocity, the longer the breakthrough time. The predicted values from the Glueckauf LDF model, Eq. (5), correspond relatively well with the experimental results. When a large fraction of the bed is covered by the concentration wave front in step II, a small fraction of the bed at the end is available for adsorption of CO_2 in the following cocurrent blowdown. Consequently, little CO_2 is desorbed, and the CO_2 concentration in the gas phase is not increased. The breakthrough time does not decrease linearly according to the linear increase in the feed velocity. And it is confirmed that the difference of the breakthrough time between 2 and 3 LSTP (Liter at Standard Temperature and Pressure)/min become larger than that between 3 and 4 LSTP/min. This implies that at least a certain amount of contact time is required due to the mass transfer resistance in the adsorbent and that for the adsorption capacity it is more efficient to operate at the 2 LSTP/min feed velocity rather than at 4 LSTP /min.

2-2. The Effects of Pressure on Breakthrough Curves

Fig. 5 shows the breakthrough curves according to the change of pressure at 2 LSTP/min. The higher the pressure, the higher the adsorption capacity and the longer breakthrough time becomes. However, at 16 atm, there is not as much elongation effect of the breakthrough time compared to that of 11 atm. This implies that it has come near the maximum amount adsorbed at equilibrium. A lower pressure in step II will favor CO_2 product purity but decrease the throughput or the productivity.

Based on the results of these preliminary breakthrough experiments, the cyclic PSA experiments are conducted at the following operating conditions: feed velocity of 2 LSTP/min at adsorption pressure of 11 atm.

2-3. The Desorption Experiment by Purge

Fig. 6 and 7 show the results of the purge step which is part of the desorption step in the five-step cyclic PSA process. Fig. 6 shows the desorption curves of H_2 of a bed saturated by H_2 at 1 atm. He is used as the purge gas for this experiment. In the case of H_2, the amount adsorbed at equilibrium is small and

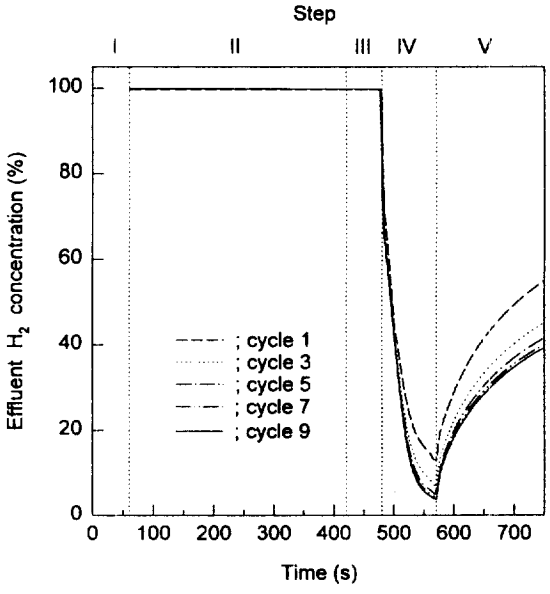

Fig. 8. Transient cyclic behavior of five-step PSA process predicted by LDF model for run A.

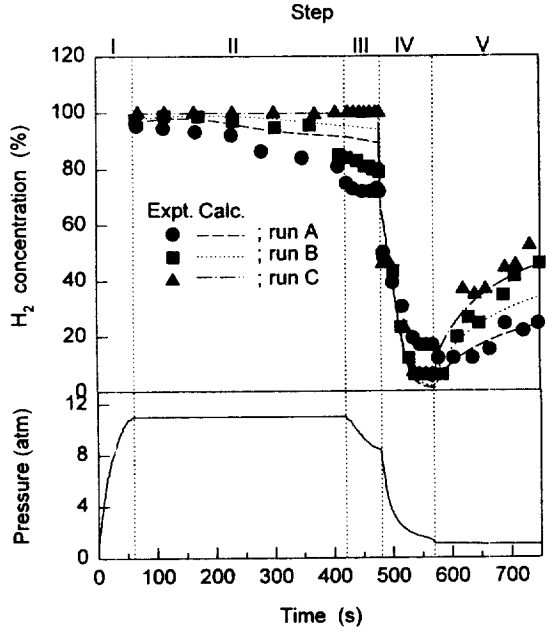

Fig. 9. Steady state results of five-step PSA separation with several P/F ratio (run A: 0.029, run B: 0.052, run C: 0.1) at 11 atm of adsorption pressure and 2 LSTP/min of feed rate.

the desorption is done in a short period of time as well. As the velocity of the carrier gas is increased, the desorption is done even in a shorter period of time. The solid curves show the predicted results by the LDF model. It is considered that the desorption curve shows a steep slope and the desorption completed quickly because of the fact that the effective diffusivity of H_2 is large and the amount adsorbed at equilibrium on zeolite 5A is small. In the case of CO_2, as shown in Fig. 7, the desorption takes longer time because of the larger adsorption capacity as well as the lower effective diffusivity.

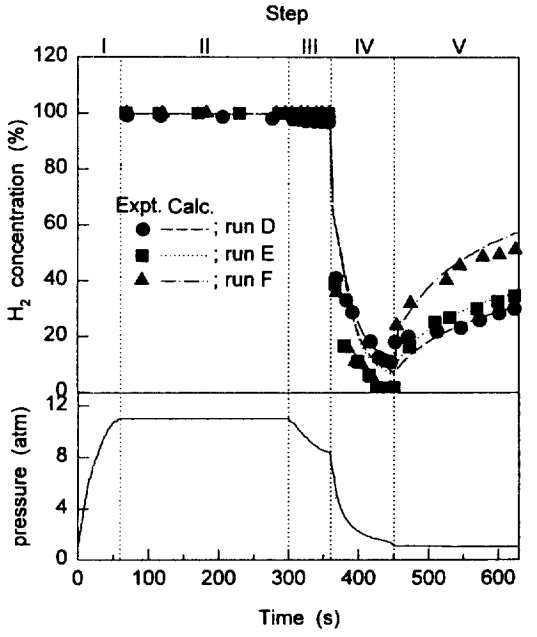

Fig. 10. Steady state results of five-step PSA separation with several P/F ratio (run D: 0.029, run E: 0.052, run F: 0.1) at 11 atm of adsorption pressure and 2 LSTP/min of feed rate.

3. Five Steps PSA Results

The five steps PSA cycle experiments are carried out at varying adsorption time and purge to feed (P/F) ratio. The cocurrent depressurization step, which could be employed to enhance the purity of the raffinate, is employed here to simulate the pressure equalization step which is usually employed in commercial multibed PSA processes. The PSA for the separation of H_2/CO_2 mixture is conducted at the following conditions: the adsorption pressure at 11 atm, the feed velocity of 2 LSTP/min, and the end pressure at the cocurrent depressurization of 8.4 atm.

In case of model simulation, the complete cyclic steady state is usually reached after about 10 cycles. Fig. 8 shows a transient cyclic behavior of effluent H_2 composition predicted by the LDF model for run A. The values predicted by the LDF model predict the behavior of all steps in PSA fairly well, considering the complexity of the process.

3-1. The Effects of P/F Ratio

The purge/feed ratio is defined as the rate of the amount of purge to the amount of feed, measured at the same conditions [Yang, 1987]. Fig. 9 shows the concentration of H_2 which is sampled at the product line for steps II and III and at the bottom exhaust line for steps IV and V. The pressure profile at every stage on run A to C is also shown at the bottom in the Fig. 9. As one can see in the figure, on run A to C with the adsorption time being 360 s, as the P/F ratio increases from 0.029 to 0.100, the purity of H_2 in the product increases, but the purity of CO_2 decreases because of dilution by the purge stream. On the other hand, as the P/F ratio increases the recovery of H_2 decreases, but that of CO_2 increases. Fig. 10 shows the concentration changes for run D to F. Similarly, for run D to F whose the adsorption time is 240 s, as P/F ratio increases, the recovery of H_2 decreases and that of CO_2 increases as before. Fig. 11 shows the effects of P/F ratio on the purity and recovery. The product purity increases with the P/F ratio in an asymptotic manner with corre-

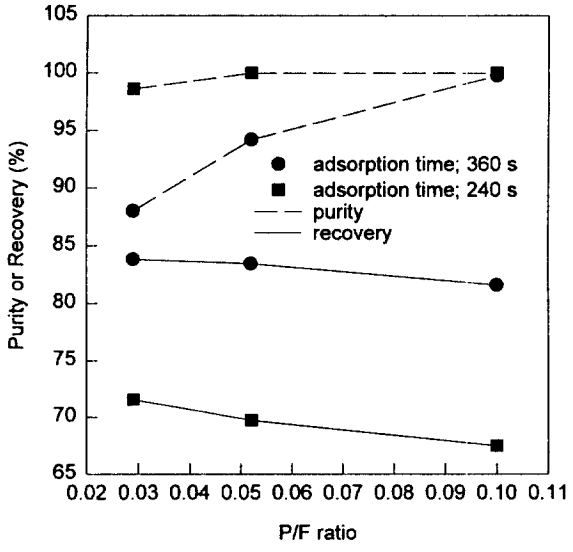

Fig. 11. Effects of the P/F ratio on recovery and purity.

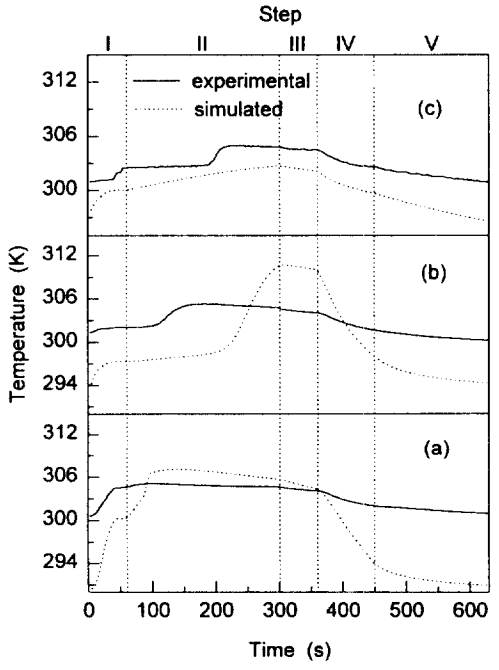

Fig. 12. Steady state temperature excursions for run E at three points [(a): 10 cm, (b): 50 cm, (c): 80 cm] from the feed end.

sponding loss of recovery. Beyond a certain range of P/F ratio the purity levels off.

In summary, as P/F ratio increases, the purity of the light product (weak adsorbate) increases with decrease of recovery but that of the heavy product (strong adsorbate) decreases. Therefore, the desired purity (and the corresponding recovery) dictates the optimum P/F ratio. It is seen from the results that a P/F ratio between 0.05 and 0.1 is a likely optimal value under the condition of 2 LSTP/min of feed rate, 11 atm of adsorption pressure, and 240 s of adsorption step time. The model is also capable of predicting such an optimal value. Table 4 shows the experimental and predicted results of the step purity, overall purity, and overall recovery.

3-2. The Effects of the Adsorption Time

When experimental results of runs A to C (longer adsorption time) are compared with those of runs D to E (shorter adsorption time) in Table 4, it is obvious that the shorter adsorption time gives the higher H_2 purity but the lower H_2 recovery. However, in the case of the bottom (heavy) product, i.e. CO_2, the shorter adsorption time gives the higher purity as well as the higher recovery.

Compared with these experimental results, the predicted values match significantly better with the experimental values at the shorter adsorption time. At the longer adsorption time (runs A, B, and C), the poor match may be due to partial breakthrough of the mass transfer zone during the cocurrent depressurization and/or the blowdown/purge steps.

In any case, the optimum adsorption time in a PSA process is a function of the bed length of the adsorber and the operating conditions, and has a great effects on the purity/recovery of the product(s).

3-3. The Effects of Temperature

The main feature in bulk separation by PSA, in contrast to purification, is the large temperature excursions encountered during each step of the cycle. The temperature histories of the bed are helpful in understanding the dynamics of the process. A practical utility of these data is the indication of the location of the wave front of the strong adsorbate (CO_2). The experimental temperature histories at three points within the bed during a steady-state cycle in run E are shown in Fig. 12, along with the model

Table 4. Experimental and predicted cyclic steady results for PSA processes

	run A	run B	run C	run D	run E	run F
P/F ratio	0.029	0.052	0.100	0.029	0.052	0.100
Step purity (%) based H_2						
step II	89.47(95.17)	95.36(97.95)	99.77(99.92)	98.69(99.67)	99.98(99.87)	99.99(99.98)
step III	73.14(90.45)	82.54(94.73)	99.69(99.84)	97.20(99.57)	99.92(99.79)	99.93(99.98)
step IV	40.42(23.34)	36.89(23.94)	35.88(25.84)	34.72(32.97)	23.54(31.32)	29.73(36.85)
step V	16.39(13.87)	27.77(20.66)	40.84(29.76)	22.85(19.71)	25.40(23.73)	40.62(40.39)
Overall purity (%)						
H_2	88.01(94.98)	94.20(97.83)	99.76(99.92)	98.61(99.67)	99.98(99.86)	99.99(99.98)
CO_2	66.06(80.55)	66.91(77.70)	61.51(72.03)	67.78(72.19)	67.10(71.65)	66.00(61.47)
Overall recovery (%)						
H_2	83.81(88.25)	83.43(85.54)	81.56(83.62)	71.55(73.71)	69.73(71.62)	67.50(69.26)
CO_2	58.22(90.25)	67.37(92.54)	76.98(93.78)	88.80(85.00)	91.31(88.49)	92.70(92.64)

( ): Predicted value

predictions by using the isosteric heat of adsorption obtained from the adsorption isotherm. The results of the comparison is quantatively not very good. The predicted results show that the temperature excursion between 290 K and 312 K while experimental results are between 300 K and 306 K.

In Fig. 12, there is a peak (or a hump) in the temperature profile which correspond to the concentration wave front, caused by the heat of adsorption. Although the movement of the position of the peak through the bed does match qualitatively, the height of the experimental peak is less significant than the simulation one.

This is interpreted to be mainly due to the following two reasons. The first reason, it seems, is that the assumption of thermal equilibrium in the modeling (No. 4) is not attained in reality. Although the rate of heat transfer in a fixed bed adsorption is known to be faster than the rate of mass transfer, it is by no means instantaneous, and therefore the actual peak is lower. The second reason is due to the thermal effect of the metal column, which is neglected in the modeling.

In a large, industrial adsorber, the thermal capacity of the metal wall is insignificant compared with that of the adsorbent. However, in a small, laboratory scale unit the thermal capacity of the wall can not be neglected in comparison with that of the adsorbent. Therefore, the heat transferred to the metal wall will have an effect to diffuse the thermal peak caused by the heat of adsorption.

Also, there is a publication which found the estimation of temperature profile for CO_2 adsorption in a PSA process by a mathematical model to be difficult [Doong and Yang, 1986].

CONCLUSIONS

Experimental results have shown that a PSA can be used as an effective process for bulk separation of H_2/CO_2. To study on the adsorption column dynamics and a cyclic PSA process, various experiments such as adsorption, desorption, and cyclic PSA processes are separately performed. In addition, adsorption equilibrium data and uptake curves are obtained to provide the data necessary for simulation of dynamics of column and PSA processes.

The role of operating parameters of PSA processes such as P/F ratio and adsorption step time is studied. The P/F ratio and adsorption step is crucially important for high H_2 purity and recovery. When the P/F ratio increases, the purity of H_2 product and the recovery of CO_2 product is increased. However, the effects of P/F ratio are not as significant for the short period time of adsorption step. High purity H_2 product can be produced by reducing the adsorption step time. At low P/F ratio, the adsorption step time does not give any significant effects for CO_2 purity, but the recovery of CO_2 is significantly increased by reducing the adsorption step time.

The experimental data of a single column PSA cycle can be simulated by a model incorporating the loading ratio correlation (LRC), heat balance equation and the linear driving force (LDF) model. Although the assumption of thermal equilibrium is found less than satisfactory, the LDF model is found to be simple and generally acceptable for representation of the adsorption dynamics in PSA process.

ACKNOWLEDGMENT

The authors wish to thank Sunkyong Engineering & Construction, Ltd., Yukong, Ltd. and R & D management center for energy resources for financial assistance and support.

NOMENCLATURE

B_i : Langmuir constant [atm^{-1}]
C_i : concentration of component i in bulk phase [mol/cm^3]
C_{pg} : heat capacity of gas mixture [cal/g·K]
C_{ps} : heat capacity of adsorbent [cal/g·K]
D_c : effective diffusivity in zeolite pellet defined by solid diffusion model [cm^2/s]
D_i : inside diameter of the column [cm]
D_o : outside diameter of the column [cm]
$\overline{D}_L$: logarithmic mean diameter of the column [cm]
h_i : heat transfer coefficient for inside of the bed [$cal/cm^2 \cdot K \cdot s$]
h_o : heat transfer coefficient for outside of the bed [$cal/cm^2 \cdot K \cdot s$]
k_1 : parameter of q_{mi} in Eq. (5) [mmol/g]
k_2 : parameter of q_{mi} in Eq. (5) [mmol/g·K]
k_3 : parameter of B_i in Eq. (5) [atm^{-1}]
k_4 : parameter of B_i in Eq. (5) [K]
k_5 : parameter of n_i in Eq. (5)
k_6 : parameter of n_i in Eq. (5)
L : column length [cm]
n_i : parameter of Eq. (5)
P : total pressure [atm]
q : amount adsorbed [mol/g]
q^* : equilibrium amount adsorbed [mol/g]
$\overline{q}$: volume-average amount adsorbed in a pellet [mol/g]
Q : average isosteric heat of adsorption [cal/mol]
r : radial distant in zeolite pellet [cm]
R : gas constant [cal/mol·K]
R_p : radius of pellet [cm]
R_{Bi} : inside radius of the column [cm]
R_{Bo} : outside radius of the column [cm]
t : time [s]
T_o : temperature of atmosphere [K]
T : pellet or column temperature [K]
u : superficial velocity [cm/s]
U_i : overall heat transfer coefficient based on inside area [$cal/cm^2 \cdot K \cdot s$]
x_w : thickness of the column wall [cm]
y_i : mole fraction of species i
z : axial distance in column from the inlet [cm]

Greek Letters

α : interpellet void fraction
α' : total void fraction
ε_a : macropore void fraction
ε_c : intracrystal void fraction
ρ_g : gas density [g/cm^3]
ρ_B : bulk density [g/cm^3]
ω : weight fraction of crystals

REFERENCES

Carter, J. W. and Wyszynski, M. L., "The Pressure Swing Adsorption Drying of Compressed Air", *Chem. Eng. Sci.*, **38**, 1093

(1983).

Cen, P. and Yang, R. T., "Bulk Gas Separation by Pressure Swing Adsorption", *Ind. Eng. Chem. Fundam.*, **25**, 758 (1986).

Cheng, H. C. and Hill, F. B., "Recovery and Purification of Light Gases by Pressure Swing Adsorption in Industrial Gas Separation", *ACS Symp. Ser.*, **223**, 195 (1983).

Doong, S.-J. and Yang, R. T., "Bulk Separation of Multcomponent Gas Mixtures by Pressure Swing Adsorption: Pore/Surface Diffusion and Equilibrium Models", *AIChE J.*, **32**, 397 (1986).

Farooq, S. and Ruthven, D. M., "Numerical Simulation of a Kinetically Controlled Pressure Swing Adsorption Bulk Separation Process Based on a Diffusion Model", *Chem. Eng. Sci.*, **46**, 2213 (1991).

Fernandez, G. F. and Kenney, C. N., "Modeling of the Pressure Swing Air Separation Process", *Chem. Eng. Sci.*, **38**, 827 (1983).

Glueckauf, E., "Theory of Chromatography. Part 10-Formula for Diffusion into Spheres and Their Application to Chromatography", *Trans. Faraday Soc.*, **51**, 1540 (1955)

Huang, C. C. and Fair, J. R., "Study of the Adsorption and Desorption of Multiple Adsorbates in a Fixed Bed", *AIChE J.*, **34**, 1861 (1988).

Kapoor, A. and Yang, R. T., "Kinetic Separation of Methane-Carbon Dioxide Mixture by Adsorption on Molecular Sieve Carbon", *Chem. Eng. Sci.*, **44**, 1723 (1989).

Kikkinides, E. S., Yang, R. T. and Cho, S. H., "Concentration and Recovery of CO_2 from Flue Gas by Pressure Swing Adsorption", *Ind. Eng. Chem. Res.*, **32**, 2714 (1993).

Liow, J. L. and Kenney, C. N., "The Backfill Cycle of the Pressure Swing Adsorption Process", *AIChE J.*, **36**, 53 (1990).

Lu, Z. P., Loureiro, J. M., Le Van, M. D. and Rodrigues, A. E., "Intraparticle Convection Effect on Pressurization and Blowdown of Adsorbers", *AIChE J.*, **38**, 857 (1992).

Ritter, J. A. and Yang, R. T., "Pressure Swing Adsorption: Experimental and Theoretical Study on Air Purification and Vapor Recovery", *Ind. Eng. Chem. Res.*, **30**, 1023 (1991).

Ruthven, D. M., Farooq, S. and Knaebel, K. S., "Pressure Swing Adsorption", VCH publisher, Inc., 1994.

Ruthven, D. M., "Principles of Adsorption and Adsorption Processes", John Wiley & Sons, New York, 1984.

Skarstrom, C. W., "Use of Adsorption Phenomenon in Automatic Plant Type Gas Analyzers", *Ann. NY Acad. Sci.*, **72**, 751 (1959).

Stewart, H. A. and Heck, J. L., "Pressure Swing Adsorption", *Chem. Eng. Progress*, **65**, 78 (1969).

Wankat, P. C., "Large-Scale Adsorption and Chromatography", CRC Press, Boca Raton, 1986.

Yang, R. T., "Gas Separation by Adsorption Processes", Butterworths, 1987.

Yang, R. T. and Doong, S. J., "Gas Separation by Pressure Swing Adsorption: A Pore-Diffusion Model for Bulk Separation", *AIChE J.*, **31**, 1829 (1985).